J. Plasma Physics (2010), *vol.* 76, *part* 5, *pp.* 699–707.
doi:10.1017/S0022377809990511

Variation of axial and radial temperature in an expanded thermal plasma jet

B. BORA[1], M. KAKATI[2] and A. K. DAS[3]

[1]Centre of Plasma Physics, Sonapur 782 402, Assam, India
[2]Thermal Plasma Processed Materials Laboratory, Department of Physics, Dibrugarh University, Dibrugarh, Assam 786 004, India
(mayurkak@rediffmail.com)
[3]Laser and Plasma Technology Division, BARC, Mumbai 400 085, India

(Received 25 January 2009 and accepted 25 November 2009, first published online 15 January 2010)

Abstract. The distribution of temperature in an expanded thermal plasma jet is investigated by modified Langmuir probes. The validation of classical probe theory in the entire experimental chamber pressure range of 10–100 mbar is thoroughly established before the measurements. The average temperature of the plasma jet at the nozzle exit was also measured by calorimetric estimation of total heat loss from the plasma upstream of that point. A correlation is made using simple analytical expression in between the average temperature measured from the heat loss data and the centerline temperature at the nozzle exit measured by Langmuir probe. The *profile parameter n* for the radial distribution of temperature in a plasma jet is calculated for different operating current and gas flow rates.

1. Introduction

Expanded thermal plasma jets have great importance in diverged branches of material processing, for example, in synthesis of nanomaterials [1], low-pressure plasma spray coating [2], chemical vapor deposition [3], thermal plasma-assisted nitriding [4], *etc*. A segmented torch-generated plasma supersonic plasma jet has been also very successfully used to simulate Tokamak Divertor-like conditions and study plasma surface interaction processes [5]. They are also used to mimic some important astrophysical phenomena [6]. In the laboratory of the authors of this paper, a similar uniformly expanded plasma beam has been used to develop a 10 $\mathrm{MW\,m^{-2}}$ level heat source for material testing. The advantage of using a subsonically expanded plasma beam to synthesize nanoparticles with a more uniform size distribution was first demonstrated by Rao *et al.* [7]. Very recently we have also synthesized oxide and nitride nanoparticles by the plasma expansion method, and established that product particles had a narrower size dispersion compared to that found in other conventional plasma-assisted attempts [8].

For proper optimization of the expanded plasma-assisted techniques and their control, it is important that the basic expansion process may be also thoroughly studied. Expanded plasmas under different operating conditions have been already investigated by advanced diagnostics techniques like Thomson–Rayleigh scattering [9], optical emission spectroscopy [10], mass spectrometry [11], *etc*. There has also been a great deal of interest in the theoretical modeling of the expanded jet from

the perspective of ultimate process optimization [12]. For easy development of the technologies it is important that cheap and easily accessible diagnostics methods are developed/employed. In this communication we report two very simple techniques for detailed characterization of a supersonic plasma beam beyond the exit of a converging nozzle. We have measured axial and radial distribution of temperature in the expanded jet with a modified Langmuir probe. Temperature measurements in the expanded region are of special interest as particle–plasma interactions occur in this region. The average temperature just outside the nozzle is measured by calorimetric heat balance calculations.

Langmuir probes are widely used in low-density plasmas to measure the electron temperature and density. However, they are rarely used in thermal plasmas because of the high heat load and highly collisional regime. Putting a probe momentarily inside an expanded plasma is relatively easier as the total heat transfer from the rarified beam is much smaller. Gindrat had studied an expanded plasma beam in the pressure range of 2–10 mbar with Langmuir probe [13, 14]. He had validated the use of the classical Langmuir theory for interpretation of the probe data for the range of his experimental chamber pressure values. In this communication, we have reported measurement of plasma parameters at a relatively high-pressure range of 20–100 mbar. In this case the shocks are compressed very close to the nozzle and we have performed measurements beyond that point only. To our knowledge nobody has explored this pressure range of expanded plasma with a simple Langmuir probe. We have also made a detailed investigation on the validity of the probe theory in this higher pressure range, using the same procedure as Gindrat [13, 14].

The average plasma temperature at the exit point of the nozzle was estimated through calorimetric measurement of heat loss from the plasma upstream of these axial locations [7, 8]. The power in the plasma gas at those sections was measured and the standard enthalpy–temperature look-up tables provided the average plasma temperature.

2. The experimental set-up

The segmented wall stabilized plasma torch used in this experiment consists of a water-cooled thoriated tungsten cathode and a water-cooled copper anode separated by water-cooled floating copper rings. The plasma is allowed to expand through a converging nozzle in to a low-pressure chamber. The full system was described in more detail in our earlier report [8]. The probe is made of a tungsten wire of 0.12 mm radius protruding 2.5 mm from an alumina cemented jacket which is quickly swept radially through the expanded plasma jet in order to reduce the total heat load. The probe is biased by a 50 Hz sine wave voltage and the output is fed to a computer through an ADVANTECH-made PCL-1800 (330 KHz, 12-bit) data acquisition card. The acquisition software is developed in visual basic, which can be viewed real time, i.e. voltage, current in the y-axis and time in the x-axis. The torch was operated with total 6 rings, argon as the plasma gas, current values for 100, 150, 200, 250 A and three different gas flow rates 10, 15, 20 liters per minute (lpm).

Each segment of the torch system is water cooled by individual water lines, from a central closed loop water circulating system. Heat rejected at the individual sections

https://doi.org/10.1017/S0022377809990511 Published online by Cambridge University Press

Table 1. Calculated Debye length and mean free path assuming LTE for different pressure and electron temperature.

P (mbar)	T_e (eV)	n_n (m^{-3})	n_e (m^{-3})	λ_D (mm)	R_p (mm)	λ_{en} (mm)
20	0.2	6.3×10^{22}	1.79×10^{11}	**7.850**	0.12	0.686
20	0.3	4.2×10^{22}	4.72×10^{16}	0.019		1.030
20	0.5	2.53×10^{22}	1.2×10^{21}	0.0001		1.716
60	0.2	1.89×10^{23}	3.10×10^{11}	**5.965**		0.228
60	0.3	1.26×10^{23}	8.18×10^{16}	0.014		0.343
60	0.5	7.59×10^{22}	2.14×10^{21}	0.0001		0.572
100	0.2	3.16×10^{23}	4.0×10^{11}	**5.25**		0.137
100	0.3	2.11×10^{23}	1.05×10^{17}	0.013		0.206
100	0.5	1.26×10^{23}	2.76×10^{21}	0.0001		0.343

is determined by measuring increase in temperature of the circulating water. AD590 temperature sensors are used for this purpose.

3. Validation of probe theory

Validity of the classical probe theory depends on the probe geometry, the sheath dimensions and the collision mean free path in the plasma. For sheaths thin compared to the probe radius, the probe geometry is almost planar and hence the plane probe theory can be applied [15]. Probe sheaths are often assumed to be of the order of Debye length $\lambda_D = 7430(T_e/n)^{1/2}$ (in meters) where T_e is the electron temperature in electron volts (eV) and n is the density (particles m^{-3}). For thin sheath the probe dimension (radius) R_p should be larger than the Debye length $\lambda_D (R_P \gg \lambda_D)$.

Probe behavior differs significantly between situations where collisions can be ignored and those where they cannot. The classical Langmuir probe theory can be used only in collision-less sheath, i.e. the mean free path λ_{en} should be larger than the probe radius ($\lambda_{\text{en}} \gg R_p$). The classical Langmuir probe theory is valid in thin sheath, collision-less situation, that is $\lambda_{\text{en}} \gg R_p \gg \lambda_D$. We have explored these conditions under our operating conditions.

Here, the Debye length has been calculated for electron temperature between 0.2 and 0.5 eV, neutral gas densities from 2.53×10^{22} to 3.16×10^{23} which corresponds to working pressure 20–100 mbar and presented in Table 1. Assuming local thermal equilibrium (LTE), the electron density at a particular temperature and pressure is calculated by using Saha's equation. The electron-neutral mean free paths (λ_{en}) have been estimated by considering the relevant collisional cross-sections.

4. Results and discussion

From Table 1, it is seen that the thin-sheath condition ($R_p \gg \lambda_D$) is valid for all high electron temperature cases. In general sheath thickness increases with temperature, but in this case the electron density increases more rapidly with temperature, thus offsetting the former effect. The other condition for application of classical Langmuir theory that is low collisionality ($\lambda_{\text{en}} \gg R_p$) is seen to be favored also in the high temperature regime. We have therefore confined our probe measurements up to a distance of 18 cm from the nozzle, and not beyond 100 mbar pressure. Figure 1 shows the measured electron temperature at different equidistant points along the jet axis, for different plasma current and gas flow rates. Temperature increases both

https://doi.org/10.1017/S0022377809990511 Published online by Cambridge University Press

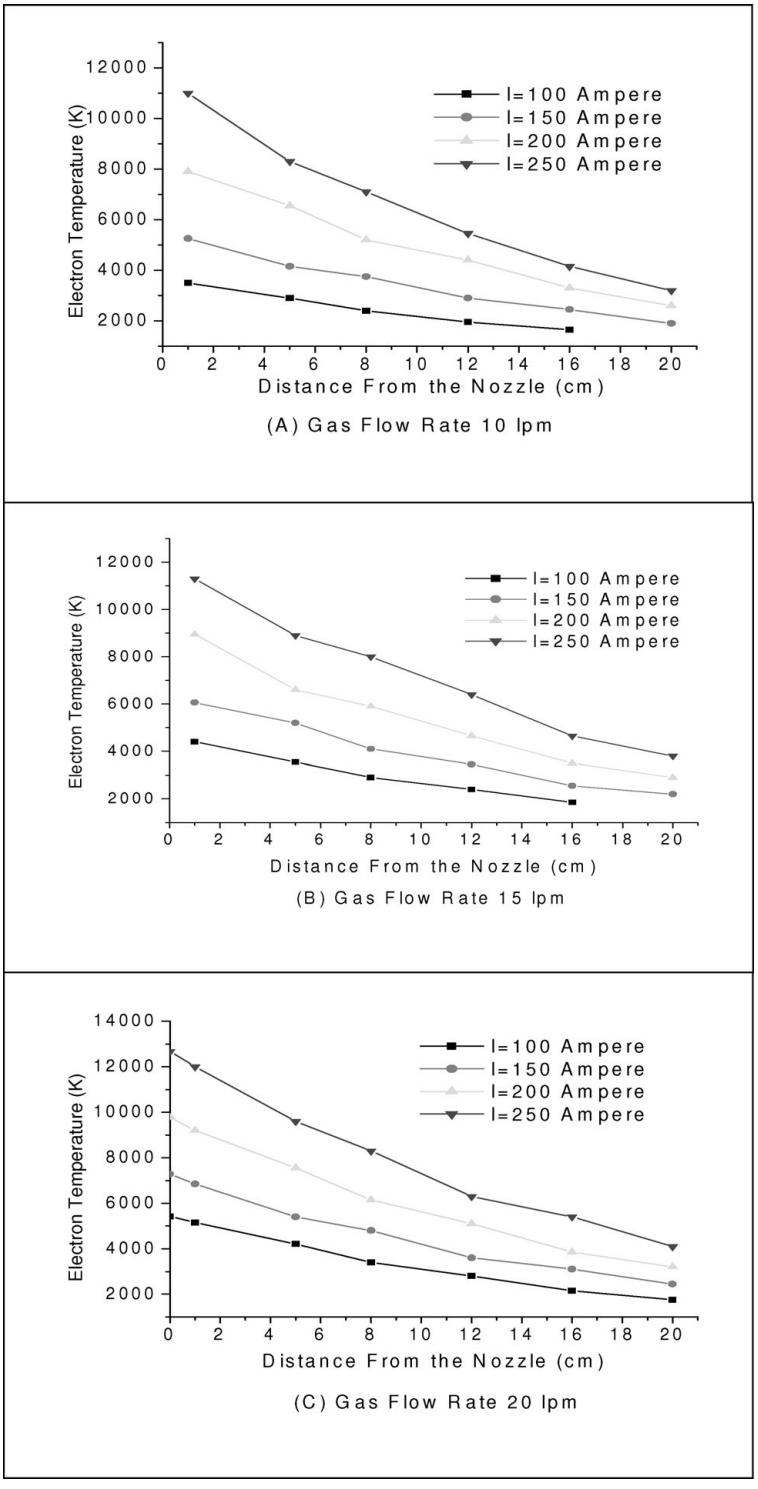

Figure 1. Variation of temperature along the jet axis for different plasma current, for (A) 10 lpm, (B) 15 lpm and (C) 20 lpm argon gas flow rate.

https://doi.org/10.1017/S0022377809990511 Published online by Cambridge University Press

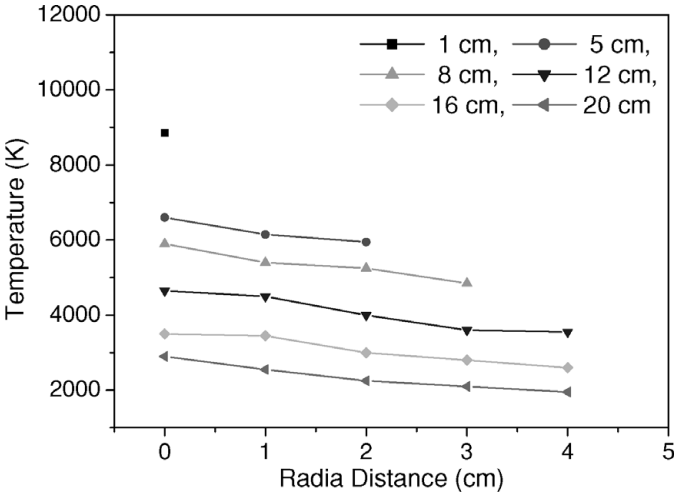

Figure 2. Radial distribution of temperature at different axial positioned for 200 A plasma current and 15 lpm gas flow rate.

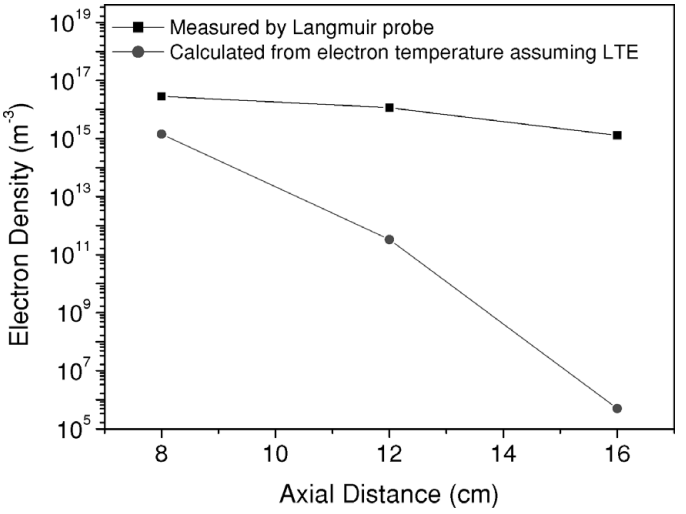

Figure 3. Electron density with axial distance, measured with Langmuir probe that predicted by Saha's equation from electron temperature.

with current and flow rate. The later fact also indicates that efficiency of the plasma torch, that is fractional amount of heat available outside the torch body, increases with the argon flow rate. The radial variation of electron temperature, at 15 lpm argon flow and 200 A plasma current, is shown in Fig. 2. This shows that beyond a certain distance from the nozzle, the temperature is almost uniform across the cross-section of the expanded plasma beam.

Figure 3 shows the Langmuir probe measured electron density in almost similar argon–nitrogen expanded plasma jet operated at 220 A of current. It is seen that the electron density actually decreases much slowly, contrary to what equilibrium calculations would predict. This was also reported in our previous report and it was concluded that this non-equilibrium electron density appeared because of the

https://doi.org/10.1017/S0022377809990511 Published online by Cambridge University Press

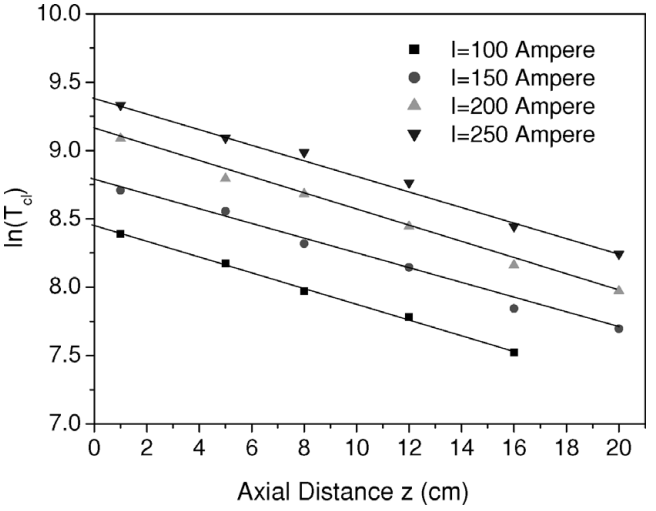

Figure 4. Plot of $\ln(T_{cl})$ versus axial distance z at 15 lpm gas flow rate.

supersonic expansion of the plasma. This observation also indicates that while calculating the validity regime of the Langmuir probe we had underestimated the electron density values. Hence, the actual sheath thickness would be smaller than that calculated in Table 1 and this has the positive effect of extending the overall validity of our Langmuir probe measurements deep down along the expanded plasma jet.

The temperature variation, axially (z) and radially (r), outside the nozzle of a thermal plasma torch may be written as [16, 17]

$$T(z,r) = T_{cl}(z)T(r),$$

where $T_{cl}(z)$ is the jet central axis temperature at a distance z from the nozzle exit and $T(r)$ is the radial distribution function for temperature which can be expressed as [16,17]

$$T(r) = 1 - \left(\frac{r}{R}\right)^n.$$

Here R is a characteristic length, which is the measure of the width of plasma jet. n is the profile parameter, which is a measure of the sharpness of variation.

The variation of centerline temperature along the axis of a plasma jet is given as

$$T_{cl}(z) = T_{cl}(0)\exp\left(-\frac{Z}{L}\right),$$

where $T_{cl}(0)$ is the centerline temperature at the nozzle exit and L is the characteristic length of the plasma. The value of $T_{cl}(0)$ is dependent on various torch operating parameters.

The measurement of nozzle exit temperature by electrostatics probe is almost impossible due to a very high heat load and other experimental difficulties. However, the value of $T_{cl}(0)$ can be determined by plotting $\ln(T_{cl})$ versus z according to the above equation, which is a straight line.

A plot of $\ln(T_{cl})$ versus z for 15 lpm plasma gas flow rate is shown in Fig. 4. The centerline temperature at the nozzle exit $T_{cl}(0)$ is calculated by extrapolating the $\ln(T_{cl})$ to $z = 0$.

https://doi.org/10.1017/S0022377809990511 Published online by Cambridge University Press

Table 2. Profile parameter n for different current and gas flow rate.

Current	100 A	150 A	200 A	250 A
Gas flow rate				
10 LPM	2.2043	2.290 68	2.360 12	2.470 07
15 LPM	2.221 21	2.320 19	2.400 19	2.510 15
20 LPM	2.300 67	2.370 24	2.470 27	2.590 11

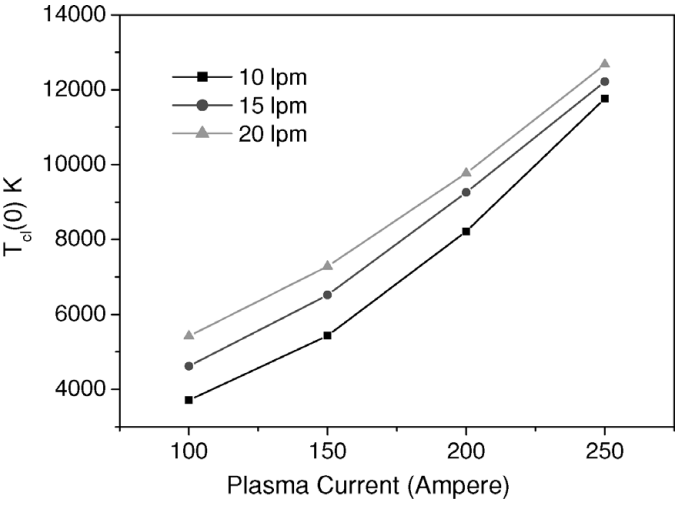

Figure 5. Centerline temperature at the nozzle exit for different current and flow rate.

The calculated centerline nozzle exit temperature by this method, for different current, is shown in Fig. 5.

Again, the average temperature $T_{av}(z)$ at any axial positioned can be given by

$$T_{av}(z) = \frac{\int_0^R T_{cl}(z)\left[1-\left(\frac{r}{R}\right)^n\right] r\, dr}{\int_0^R r\, dr}.$$

At the nozzle exit i.e. $z = 0$ and $R = R_0$ (nozzle outlet radius), the average temperature T_{av} will be

$$T_{av} = T_{cl}(0)\left(\frac{n}{n+2}\right).$$

In this experiment, the average temperature T_{av} at the nozzle exit measured by the calorimetric method is shown in Fig. 6. From these data, the profile parameter, n, for different current and flow rate is calculated by the above equation and recorded in Table 2. Joshi *et al.* had measured the value of n to lie in between 2.2 and 2.6, which is close to our calculated range [16].

5. Conclusions

The axial and radial variation of temperature of an argon plasma jet expanding supersonically into a low-pressure chamber has been measured for different current

https://doi.org/10.1017/S0022377809990511 Published online by Cambridge University Press

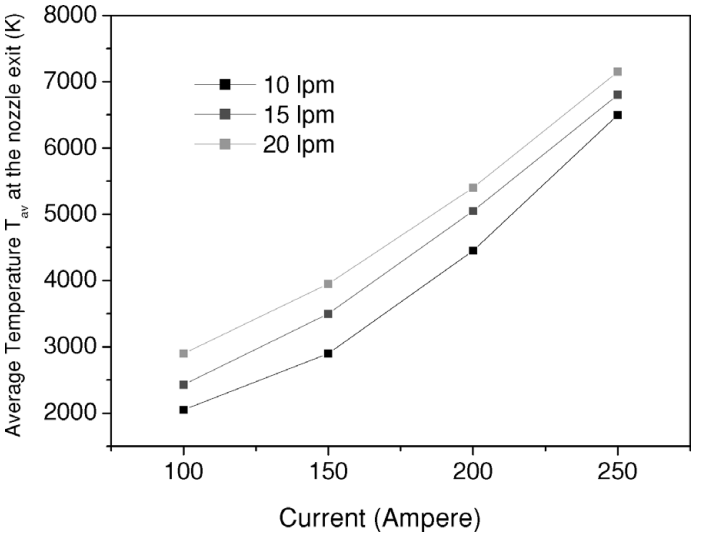

Figure 6. Average temperature at the nozzle exit measured from heat loss data.

and gas flow rates. A modified Langmuir probe has been used to characterize the expanding plasma where the emission light intensity is insufficient for optical diagnostic. It is seen that after a certain distance temperature remains almost constant across the cross-section of the plasma beam. Hence, this type of plasma is ideal for applications where a uniform temperature profile is required. Calorimetric estimation is used to find out the average temperature at the nozzle exit. The plasma jet centerline temperature is also measured using a simple extrapolation technique. We have also made an estimation for the profile parameter n, corresponding to the distribution of temperature very close to the nozzle.

References

[1] Kakati, M. and Das, A. K. 2009 *New Nanotechniques.* (ed. A. Malik and R. J. Rawat). New York: Nova Publishers, pp. 1.

[2] Han, Z., Xu, B., Wang, H. and Zhou, S. 2007 *Surf. Coat. Technol.* **201**, 5253.

[3] Han, P. and Chen, X. 2001 *Thin Solid Films* **390**, 181.

[4] Tahara, H., Ando, Y. and Yoshikawa, T. 2003 *IEEE Trans. Plasma Sci.* **31**, 281.

[5] Groot, B. de., Ahmad, Z., Dahiya, R. P., Engeln, R., Goedheer, W. J., Cardoza, N. J. L. and Veremiyenko, V. 2003 *Fusion Eng. Des.* **66–68**, 413.

[6] van den Oever, P. J., van Helden, J. H., Lamers, C. C. H., Engein, R., Schram, D. C., van de Sanden, M. C. M. and Kessels, W. M. M. 2005 *J. Appl. Phys.* **98**, 093 301.

[7] Rao, N., Girshick, S., Heberlein, J., McMurry, P., Jones, S., Hansen, D. and Micheel, B. 1995 *Plasma Chem. Plasma Process* **15**(4), 581.

[8] Kakati, M., Bora, B., Sarma, S., Sripathi, T., Deshpande, U., Dubey, A., Ghosh, G. and Das, A. K. 2008 *Vacuum* **82**, 833.

[9] Meulenbroeks, R. F. G., Engeln, R. A. H., Beurskens, M. N. A., Paffen, R. M. J., van de Sanden, M. C. M. and van der Mullen, J. A. M. 1995 *Plasma Sources Sci. Technol.* **4**, 74.

[10] Selezneva, S. E., Rajabian, M., Gravelle, D. and Boulos, M. I. 2001 *J.Phys. D: Appl. Phys.* **34**, 2862.

[11] van den Oever, P. J., van Hemmen, J. L., van Helden, J. H., Schram, D. C., Engeln, R., van de Sanden, M. C. M. and Kessels, W. M. M. 2005 *Plasma Sources Sci. Technol.* **15**, 546.

[12] Han, P. and Chen, X. 2001 *Thin Solid Films* **390**, 181.

[13] Gindrat, M., Dorier, J. L., Hollenstein, C., Refke, A. and Barbezat, G. 2004 *Plasma Sources Sci. Technol.* **13**, 484.

[14] Gindrat, M. 2004 Characterization of supersonic low pressure plasma jet. *Ph.D. Thesis*, Centre de Recherches en Physique des Plasmas, Switzerland, p. 41.

[15] Chen, F. F. 1965 *Plasma Diagnostic Techniques*. (ed. R. H. Huddlestone and S. L. Leonard) New York: Academic Press, pp. 113.

[16] Joshi, N. K., Sahasrabudhe, S. N., Sreekumar, K. P. and Venkatramani, N. 1997 *Meas. Sci. Technol.* **8**, 1146.

[17] Ghorui, S., Sahasrabudhe, S. N., Murthy, P. S. S. and Das, A. K. 2006 *Plasma Sources Sci. Technol.* **15**, 689–694.